Proceedings of Symposia in Applied Mathematics
Volume 47, 1993

Wavelets and Fast Numerical Algorithms

GREGORY BEYLKIN

into a basis and the computations take place in the new system of coordi-

In the usual transform methods, the functions of the basis (e.g. exponentials, Chebyshev polynomials, etc.) are chosen to be eigenfunctions of some differential operator (e.g. solutions of the Sturm-Liouville problem). The choice of the differential operator and, hence, of the basis functions, is dictated by the availability of fast algorithms for expanding an arbitrary function into the basis.

bases are very narrow.

Wavelets, on the other hand, are not solutions of a differential equation. These functions are defined recursively and are generated via an iterative algorithm. They are translations and dilations of a single function.[1] Instead of diagonalizing some differential operator, representations in the wavelet bases reduce a wide class of operators to a sparse form. Here the orthogonality of wavelets to the

the non-standard form (which achieves uncoupling among the scales) and the associated fast numerical algorithms. Examples of non-standard forms of several basic operators (e.g. derivatives) will be computed explicitly.

1. Multiresolution analysis and wavelets.

We briefly outline here the properties of compactly supported wavelets and refer for details to [16], [17] and [28]. Let us start with the notion of a multiresolution analysis [26], [23] which captures the essential features of all multiresolution approaches developed so far.

DEFINITION 1.1. A multiresolution analysis is a decomposition of the Hilbert space $\mathbf{L}^2(\mathbf{R}^d)$, $d \geq 1$, into a chain of closed subspaces

$$\cdots \subset \mathbf{V}_2 \subset \mathbf{V}_1 \subset \mathbf{V}_0 \subset \mathbf{V}_{-1} \subset \mathbf{V}_{-2} \subset \cdots \tag{1.1}$$

such that

(i) $\bigcap_{j \in \mathbf{Z}} \mathbf{V}_j = \{0\}$ and $\bigcup_{j \in \mathbf{Z}} \mathbf{V}_j$ is dense in $\mathbf{L}^2(\mathbf{R}^d)$.

(ii) For any $f \in \mathbf{L}^2(\mathbf{R}^d)$ and any $j \in \mathbf{Z}$, $f(x) \in \mathbf{V}_j$ if and only if $f(2x) \in \mathbf{V}_{j-1}$.

$$\mathbf{V}_n \subset \cdots \subset \mathbf{V}_2 \subset \mathbf{V}_1 \subset \mathbf{V}_0, \quad \mathbf{V}_0 \subset \mathbf{L}^2(\mathbf{R}^d) \tag{1.6}$$

instead of (1.4). In numerical realizations the subspace $\mathbf{V}_0$ is finite dimensional.

(1.9) as

$$\hat{\varphi}(\xi) = m_0(\xi/2)\hat{\varphi}(\xi/2), \tag{1.10}$$

where

(1.11) [illegible]

and the 2π-periodic function m_0 is defined as

(1.12) $$m_0(\xi) = 2^{-1/2} \sum_{k=0}^{L-1} h_k e^{ik\xi}$$

Second, the orthogonality of $\{\varphi(x-k)\}_{k\in\mathbf{Z}}$ implies that

$$\delta_{k0} = \int_{-\infty}^{+\infty} \varphi(x-k)\varphi(x)\,dx = \int_{-\infty}^{+\infty} |\hat{\varphi}(\xi)|^2 \,\mathrm{e}^{-ik\xi}\,d\xi, \tag{1.13}$$

and, therefore,

and

$$\sum_{l\in\mathbf{Z}} |\hat{\varphi}(\xi+2\pi l)|^2 = \frac{1}{2\pi}. \tag{1.15}$$

Using (1.10), we obtain

$$\sum_{l\in\mathbf{Z}} |m_0(\xi/2+\pi l)|^2 |\hat{\varphi}(\xi/2+\pi l)|^2 = \frac{1}{2\pi}, \tag{1.16}$$

and, by taking the sum in (1.16) separately over odd and even indices, we have

or, equivalently, the Fourier transform of ψ by

where

$$k=L-1$$

$$k=0$$

it is not difficult to show (see e.g., [28], [16], [17]), that for each fixed scale $j \in \mathbf{Z}$, the wavelets $\{\psi_{j,k}(x) = 2^{-j/2}\psi(2^{-j}x - k)\}_{k\in\mathbf{Z}}$ form an orthonormal basis of $\mathbf{W}_j$.

Equation (1.18) can also be viewed as the condition for exact reconstruction for a pair of the quadrature mirror filters (QMFs) H and G, where $H = \{h_k\}_{k=0}^{k=L-1}$ and $G = \{g_k\}_{k=0}^{k=L-1}$. Such exact QMF filters were first introduced by Smith and Barnwell [32] for subband coding.

We will not go into a full discussion of the necessary and sufficient conditions for the quadrature mirror filters H and G to generate a wavelet basis and refer to [17] for the details. The coefficients of the quadrature mirror filters H and G are computed by solving a set of algebraic equations (see e.g. [17]). The

with $\mathcal{M}_0 = 1$.

Alternatively, using

$$\hat{\varphi}(\xi) = (2\pi)^{-1/2} \prod_{j=1}^{\infty} m_0(2^{-j}\xi), \tag{1.27}$$

the moments $\mathcal{M}_m$ may be obtained within the desired accuracy as a limit of a

with kernel $K(x,y)$. The orthogonal projection operators on the subspace $\mathbf{V}_j$,

$j \in \mathbf{Z}$,

$$P_j : \mathbf{L}^2(\mathbf{R}) \to \mathbf{V}_j, \tag{2.3}$$

are given by

$$(P_j f)(x) = \sum_k \langle f, \varphi_{j,k} \rangle \varphi_{j,k}(x). \tag{2.4}$$

Expanding T in a "telescopic" series, we obtain

$$T = \sum_{j \in \mathbf{Z}} (Q_j T Q_j + Q_j T P_j + P_j T Q_j), \tag{2.5}$$

where

$$Q_j = P_{j-1} - P_j \tag{2.6}$$

is the projection operator on the subspace $\mathbf{W}_j$. If there is a coarsest scale n, then instead of (2.5) we have

$$T = \sum_{j=-\infty}^{n} (Q_j T Q_j + Q_j T P_j + P_j T Q_j) + P_n T P_n, \tag{2.7}$$

and if the scale $j = 0$ is the finest scale, then

$$T = \sum_{j=-\infty}^{n} (Q_j T Q_j + Q_j T P_j + P_j T Q_j) + P_n T P_n, \tag{2.8}$$

where $T \sim T_0 = P_0 T P_0$ is a discretization of the operator T on the finest scale.

The non-standard form is a representation (see [7]) of the operator T as a

where the operators T_j,

$$T_j : \mathbf{V}_j \to \mathbf{V}_j, \tag{2.14}$$

are defined by $T_j = P_j T P_j$.

If there is a coarsest scale n, then

$$T = \{\{A_j, B_j, \Gamma_j\}_{j \in \mathbf{Z}: j \le n}, T_n\}, \tag{2.15}$$

where $T_n = P_n T P_n$. If the number of scales is finite, then $j = 1, 2, \ldots, n$ in (2.15) and the operators are organized as blocks of a matrix (see Figures 1 and 2).

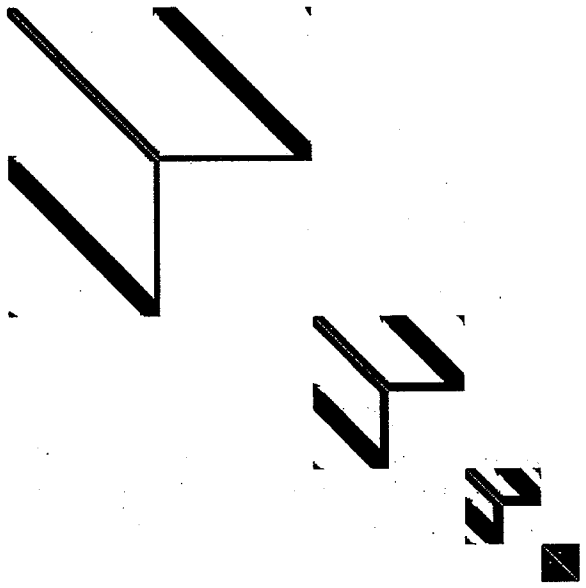

FIGURE 2. An example of a matrix in the non-standard form (see Example 4.2).

FIGURE 3. The non-standard form of the same matrix as in

$$\beta^j_{k,k'} = \int\int K(x,y)\,\psi_{j,k}(x)\,\varphi_{j,k'}(y)\;dxdy, \tag{2.17}$$

and

$$\gamma^j_{k,k'} = \int\int K(x,y)\,\varphi_{j,k}(x)\,\psi_{j,k'}(y)\;dxdy. \tag{2.18}$$

The operator T_j is represented by the matrix s^j,

$$s^j_{k,k'} = \int\int K(x,y)\,\varphi_{j,k}(x)\,\varphi_{j,k'}(y)\;dxdy. \tag{2.19}$$

3. The standard form.

The standard form is the representation of an operator in the tensor product basis. Instead of introducing the standard form in this manner, we emphasize the connection with the non-standard form. The standard form is obtained by representing

$$\mathbf{V}_j = \bigoplus_{j'>j} \mathbf{W}_{j'}, \tag{3.1}$$

and considering for each scale j the operators $\{B^{j'}_j, \Gamma^{j'}_j\}_{j'>j}$,

$$B^{j'}_j : \mathbf{W}_{j'} \to \mathbf{W}_j, \tag{3.2}$$

$$\Gamma^{j'}_j : \mathbf{W}_j \to \mathbf{W}_{j'}. \tag{3.3}$$

If there is a coarsest scale n, then instead of (3.1) we have

$$\mathbf{V}_j = \mathbf{V}_n \bigoplus_{j'=j+1}^{j'=n} \mathbf{W}_{j'}. \tag{3.4}$$

In this case, the operators $\{B^{j'}_j, \Gamma^{j'}_j\}$ for $j' = j+1, \ldots, n$ are as in (3.2) and (3.3) and, in addition, for each scale j there are operators $\{B^{n+1}_j\}$ and $\{\Gamma^{n+1}_j\}$,

$$B^{n+1}_j : \mathbf{V}_n \to \mathbf{W}_j, \tag{3.5}$$

$$\Gamma^{n+1}_j : \mathbf{W}_j \to \mathbf{V}_n. \tag{3.6}$$

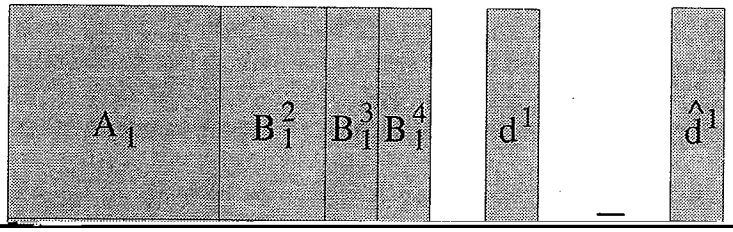
A_1
B_1^2
B_1^3
B_1^4
d^1
$\hat{d}^1$

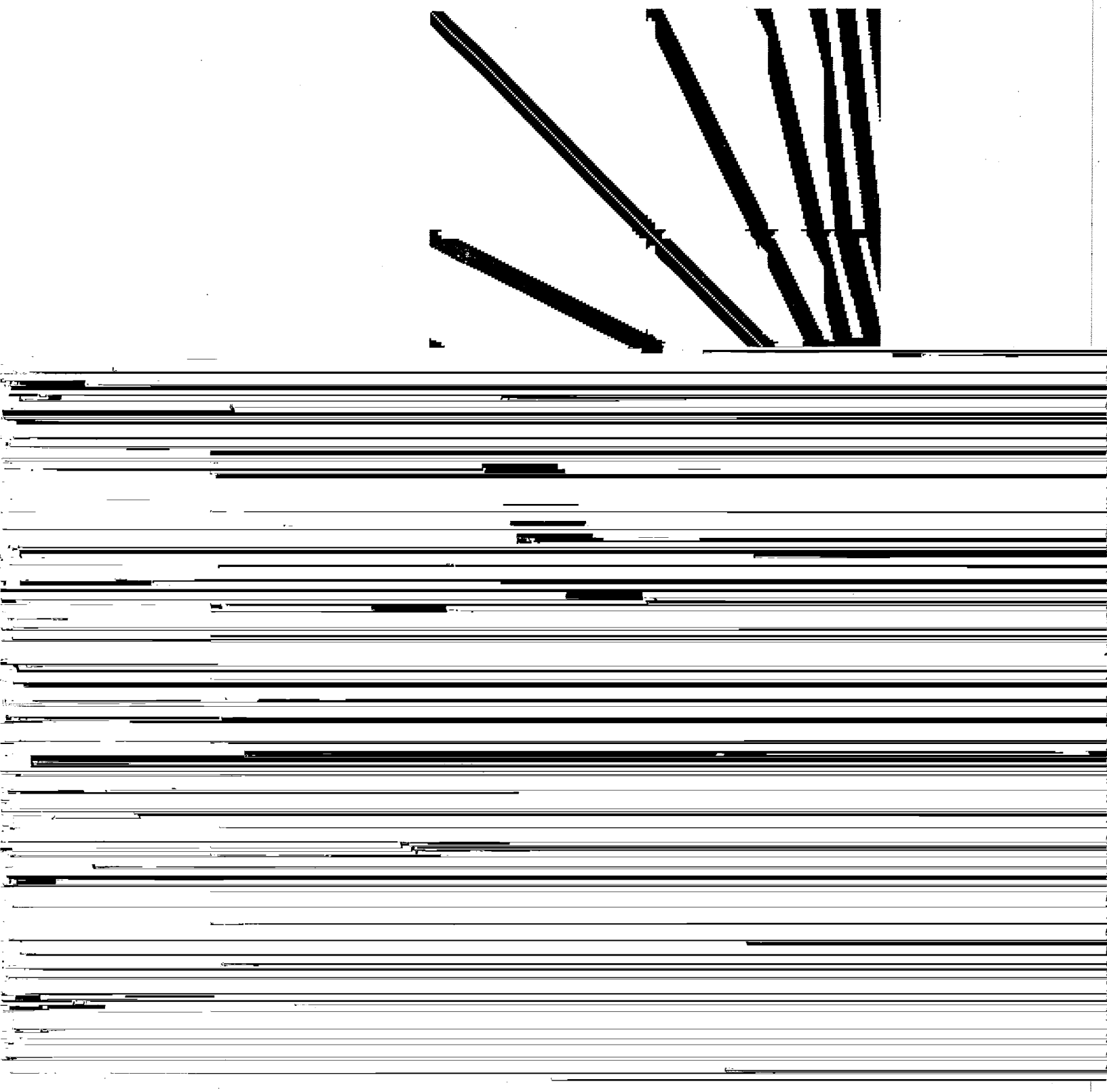

FIGURE 5. An example of a matrix in the standard form (see Example 4.2).

for some $M \geq 1$. Then by choosing the wavelet basis with M vanishing moments, the coefficients $\alpha^j_{i,l}, \beta^j_{i,l}, \gamma^j_{i,l}$ of the non-standard form (see (2.16) - (2.18)) satisfy the estimate

$$|\alpha^j_{i,l}| + |\beta^j_{i,l}| + |\gamma^j_{i,l}| \leq \frac{C_M}{1 + |i-l|^{M+1}}, \tag{4.3}$$

for all

where K is the distributional kernel of T then assuming that the symbols σ of

$$(4.7) \qquad | \partial_\xi^\alpha \partial_x^\beta \sigma(x,\xi) | \leq C_{\alpha,\beta}(1+ | \xi |)^{\lambda-\alpha+\beta}$$

$$(4.8) \qquad | \partial_\xi^\alpha \partial_x^\beta \sigma^*(x,\xi) | \leq C_{\alpha,\beta}(1+ | \xi |)^{\lambda-\alpha+\beta},$$

we have the inequality

$$(4.9) \qquad |\alpha_{i,l}^j| + |\beta_{i,l}^j| + |\gamma_{i,l}^j| \leq \frac{2^{\lambda j} C_M}{(1+|i-l|)^{M+1}},$$

for all integer i, l.

Suppose now that we approximate the operator T_0 by the operator T_0^B obtained from T_0 by setting to zero all coefficients of matrices α^j, β^j and γ^j outside

bands of width $B \geq 2M$ around their diagonals. We obtain

$$(4.10) \qquad \| T_0^B - T_0 \| \leq \frac{C}{B^M} \log_2 N,$$

where C is a constant determined by the kernel K and $\log_2 N$ is the number of scales in the representation. In most numerical applications, the accuracy ε of calculations is fixed, and the parameters of the algorithm (in our case, the band

$$\gamma(y) = T^*(1)(y) \tag{4.15}$$

satisfy the dyadic bounded mean oscillation (B.M.O.) condition,

$$\sup_J \frac{1}{|J|} \int_J |\beta(x) - m_J(\beta)|^2 dx \le C, \tag{4.16}$$

where J is a dyadic interval and

$$m_J(\beta) = \frac{1}{|J|} \int_J \beta(x) dx. \tag{4.17}$$

Again we refer to [7] for details.

The compression of operators results in fast algorithms for evaluation of operators on functions. We present here one example and refer to [7] for additional examples.

EXAMPLE 4.2. In this example, we consider the matrix

$$A_{ij} = \begin{cases} \frac{1}{i-j} & i \neq j, \\ 0 & i = j, \end{cases}$$

ments. Setting to zero all entries whose absolute values are smaller than 10^{-7}, we obtain the non-standard form where the non-zero elements are shown in black

by computing in the wavelet system of coordinates. Finally, the last column contains the compression coefficients C_{comp}, defined by the ratio of N^2 to the number of non-zero elements in the non-standard form of of the matrix.

5. The operator d/dx in wavelet bases.

[redacted]

Hilbert and Riesz transforms) we may compute the non-standard form in the wavelet bases by solving a small system of linear algebraic equations [4]. As an example, we construct the non-standard form of the operator d/dx. The matrix elements α_{il}^j, β_{il}^j, and γ_{il}^j of A_j, B_j, and Γ_j, where $i, l, j \in \mathbf{Z}$ for the operator d/dx are easily computed as

$$\int^{\infty}$$

where

$$r_l = \int_{-\infty}^{+\infty} \varphi(x-l)\,\frac{d}{dx}\varphi(x)\,dx, \quad l \in \mathbf{Z}. \tag{5.10}$$

Therefore, the representation of d/dx is completely determined by the coefficients r_l in (5.10) or in other words, by the representation of d/dx on the subspace $\mathbf{V}_0$. Rewriting (5.10) in terms of $\hat{\varphi}(\xi)$ (see (1.11)), we obtain

$$r_l = \int_{-\infty}^{+\infty} |\hat{\varphi}(\xi)|^2 (\mathrm{i}\xi) \mathrm{e}^{-\mathrm{i}l\xi}\,d\xi. \tag{5.11}$$

Thus, the coefficients r_l depend only on the autocorrelation function of the scaling function φ, rather than the scaling function itself since the integral in (5.11)

depends only on $|\hat{\varphi}(\xi)|^2$. The same holds, in fact, for all compactly

Solving equations (5.12), (5.13), we present the results for Daubechies' wavelets with $M = 2, 3$. For further examples we refer to [4].

1. $M = 2$

$$a_1 = \frac{9}{8}, \quad a_3 = -\frac{1}{8},$$

and

We note that the coefficients $(-1/12, 2/3, 0, -2/3, 1/12)$ of this example can be found in many books on numerical analysis as a choice of coefficients for numerical differentiation.

2. $M = 3$

$$a_1 = \frac{75}{64}, \quad a_3 = -\frac{25}{128}, \quad a_5 = \frac{3}{128},$$

and

$$r_1 = -\frac{272}{365}, \quad r_2 = \frac{53}{365}, \quad r_3 = -\frac{16}{1095}, \quad r_4 = -\frac{1}{2920}.$$

The structure of non-standard and standard forms of derivative operators is illustrated in Figures 6 and 7.

FIGURE 6. Sparse structure of the non-standard form of derivative operators. The width of the bands depends only on the choice of the basis and is equal to $2L - 3$.

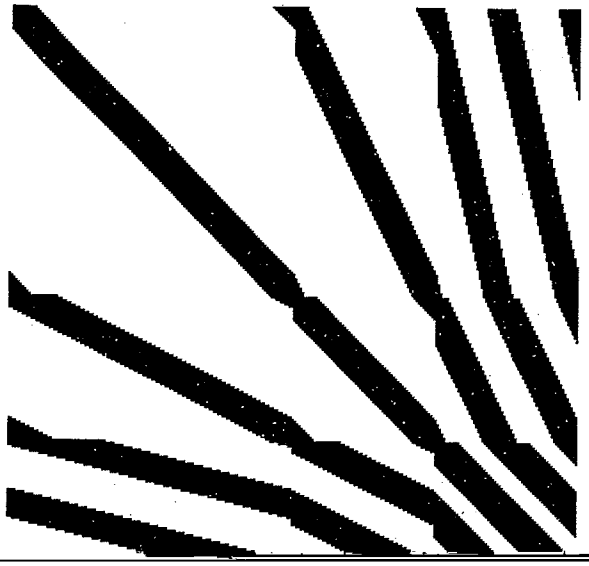

FIGURE 7. Sparse structure of the standard form of derivative operators.

For the coefficients $r_l^{(n)}$ of d^n/dx^n, $n > 1$, the system of linear algebraic equations is similar to that for the coefficients of d/dx. This

We present here two tables illustrating such preconditioning applied to the

N	κ	κ_p
64	0.14545E+04	0.10792E+02
128	0.58181E+04	0.11511E+02
256	0.23272E+05	0.12091E+02
512	0.93089E+05	0.12604E+02
1024	0.37236E+06	0.13045E+02

[redacted]

N	κ	κ_p
64	0.10472E+04	0.43542E+01
128	0.41886E+04	0.43595E+01
256	0.16754E+05	0.43620E+01

and

$$\mathcal{M}_\Phi^m = \int_{-\infty}^{+\infty} y^m \, \Phi(y) dy = 0, \quad \text{for} \quad 1 \le m \le 2M-1. \tag{5.26}$$

The vanishing moments of the autocorrelation function Φ allow us to compute the elements of the matrix $t_l^{(j)}$ for large l and sufficiently fine scales $j < 0$

Expanding the kernel K in its Taylor series, we obtain from (5.23)

$$t_l^{(j)} = 2^j K(2^j l) + \frac{(-1)^{2M} 2^{(2M+1)j}}{(2M)!} \int_{-\infty}^{+\infty} K^{(2M)}(2^j(l-\tilde{y}))\, \Phi(y)\, dy, \tag{5.27}$$

where $\tilde{y} = \tilde{y}(y,l)$ and $K^{(2M)}$ denotes the $(2M)$th derivative of K. The decay of $K^{(2M)}(2^j(l-\tilde{y}))$ for large l is faster than that of the original kernel (see (4.1) and (4.2) with an appropriate choice of M) and (5.27) is well-conditioned

algebraic equations

$$r_l = 2^\alpha \left[r_{2l} + \tfrac{1}{2} \sum_{k=1}^{L/2} a_{2k-1} (r_{2l-2k+1} + r_{2l+2k-1}) \right], \tag{5.33}$$

where the coefficients a_{2k-1} are given in (5.14). Using (5.27), we obtain the asymptotics of r_l for large l.

where A^* is the adjoint matrix and α is chosen so that the largest eigenvalue of $\alpha A^* A$ is less than one. Then the sequence X_k converges to the generalized inverse $A^\dagger$.

Combining this iteration with fast multiplication algorithms, we obtain an algorithm for constructing the generalized inverse in at most $O(N \log^2 N \log R)$ operations, where R is the condition number of the matrix. (By the condition

18. L. Greengard, *Potential flow in channels*, SIAM J. Sci. Stat. Comput. **11** (1990), no. 4, 603–620.
19. L. Greengard and V. Rokhlin, *A fast algorithm for particle simulations*, J. Comp. Phys.